Two-Dimensional 45° Surface-Normal Microcoupler Array for Guided-Wave Optical Clock Distribution

Jianhua Gan, Linghui Wu, Hongfa Luan, Bipin Bihari, and Ray T. Chen, *Member, IEEE*

***Abstract*—Surface-normal couplers are indispensable parts of a guided-wave optoelectronic interconnects for the coupling of optical signals into and out of the waveguides while facilitating the packaging. In this paper, integration of the 45° surface-normal couplers at each fanout end of the H-tree waveguide structure is described. An optical clock signal distribution system is under development using polyimide based H-tree waveguide structure. The coupler is a 45° slanted end surface of the polyimide waveguide. The coupler works for a wide range of wavelength. The experimentally estimated output coupling efficiency is nearly 100%. To determine the optimized size and shape of the photodetector, near and far field diffraction patterns are evaluated. Experimental results conclude that the phenomenon is dominated by the fundamental mode of the highly multimode waveguide.**

***Index Terms*—45° microcoupler, guided-wave optical interconnects, H-tree polyimide waveguide, optical clock distribution.**

I. Introduction

THE CLOCK skew, bandwidth limitations, cross talk and severe power budget requirement due to the skin effect are serious problems for electrical interconnects when the clock rate in the computer is pushed toward the multigigahertz range. Guided-wave optical interconnects show great potential to overcome these bottlenecks [1]. Optical interconnects for interchip and interboard level are being vigorously investigated for high data rate applications [2]–[4]. All guided-wave optoelectronic interconnection configuration involve the coupling of the light signal from the source (e.g., VCSEL) to waveguide and the coupling of it from the waveguide to photodetectors. Thus surface-normal microcoupler is a key component in planar integrated optical systems. Employment of conventional coupling techniques utilizing prisms and lenses is costly, bulky and very inconvenient from the packaging point of view and often put restriction on planarization. The waveguide grating or waveguide mirror based coupler can overcome the above problems. However, a grating based approach requires precise control of grating parameters for efficient coupling and usually have low tolerance to wavelength variations. Unlike grating couplers [5], [6], 45° surface-normal microcouplers are easy to fabricate, reproducible and relatively insensitive to wavelength variations. Here, we describe the integration of 45° microcouplers in a guided-wave clock distribution system. This guided-wave optical interconnection network is designed to be compatibly integrated onto the supercomputer boards to become an additional interconnection layer among many other electrical interconnection layers. This optical clock distribution system is capable of delivering clock signal to other chips at gigabits per second speed with a minimized clock skew.

Polyimides are widely used in silicon CMOS processing. We have used Ultradel 9120D to fabricate an H-tree waveguide, a 1-to-48 fanout structure with equivalent optical paths. 9120D is a negative-acting, photosensitive polyimide. It is characterized by high optical transparency, high thermal stability and ease of fabrication. At the wavelength of 1.310 μm, the refractive indices are 1.5364 and 1.5073 for TE and TM waves, respectively. The optical losses of the material are 1.04 dB/cm at 633 nm, 0.13 dB/cm at 830 nm, 0.09 dB/cm at 1064 nm, 0.34 dB/cm at 1300 nm and 1.21 dB/cm at 1550 nm. The glass transition temperature is 390 °C. The coefficient of thermal expansion at 300 °C is 27 ppm/°C. The moisture uptake at 100% relative humidity is 3.0%. Polyimides with lower refractive indices are also available for cladding and buffer coatings.

II. Two-Dimensional 45° Surface-Normal Microcoupler Array Fabrication

A novel board-level optical clock distribution system based on polyimide waveguides, 45° surface-normal microcouplers and fast photodetectors will be the enabling technology to boost the clock rate in supercomputer and other high performance digital systems to multigigahertz range. One major concern that needs to be addressed is the Si-CMOS process compatibility [1]. The thermal stability of polyimide renders the polyimide waveguide and microcouplers compatible with Si-CMOS process. In order to minimize the clock skew in the clock distribution system, we use an H-tree configuration to equalize the paths to all the fanout points. The schematic of a 1-to-48 H-tree structure is shown in Fig. 1.

The H-tree waveguides have been fabricated using photolithography. A silicon wafer with 2-μm-thick silicon dioxide is used as the substrate. A silicon dioxide layer acts as the buffer layer. As an alternative, other low index polyimide can also be used as cladding and buffer layers. About 10-μm-thick polyimide 9120D is spin-coated on the clean substrate. The H-tree structure is patterned to the polyimide layer using UV photolithography, and the waveguide without 45° microcouplers is obtained [7]. We use RIE to fabricate the 45° microcoupler at the end of each branch of the waveguide. The corresponding processing steps are shown in Fig. 2. A 0.3 nm-thick aluminum film is coated over the H-tree waveguides. Photoresist AZ5206E is coated over aluminum. A mask is

Manuscript received February 16, 1999; revised July 6, 1999. This work was supported by DARPA, by the BMDO, by the AFOSR, by Cray Research, by the 3M Foundation, by the Texas ATP program, and by the OIDA Joint U.S.–Japan Optoelectronics Project.

The authors are with the Microelectronics Research Center, Department of Electrical and Computer Engineering, The University of Texas at Austin, Austin, TX 78712 USA.

Publisher Item Identifier S 1041-1135(99)08685-1.

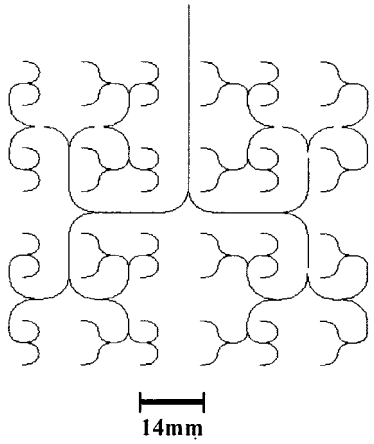

Fig. 1. 1-to-48 H-tree polyimide waveguide for optical clock distribution.

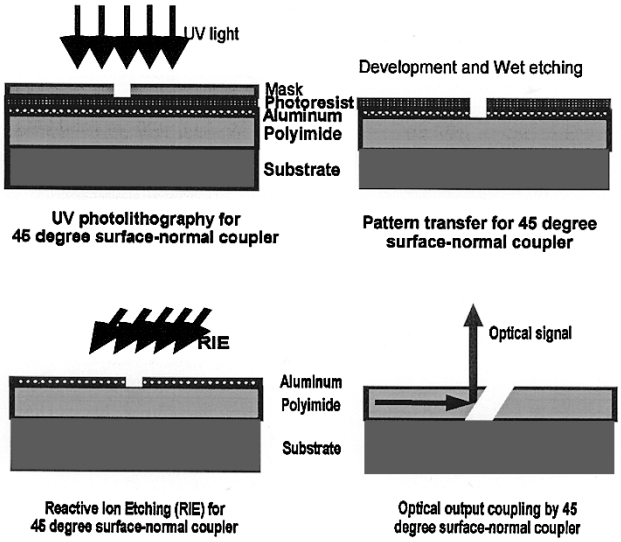

Fig. 2. The processing steps of making 45° microcoupler using RIE.

used to pattern the end portions of the 48 branches of the waveguides. The pattern is then transferred to an aluminum layer by wet etching. This opens a square window at each end of the 48 branches of the waveguide. One edge of the window is parallel to the end of the branch. The aluminum layer acts as a mask in a reactive-ion etching (RIE) chamber. The sample is mounted 45° with respect to the electrode plates of the RIE chamber. A Faraday cage [8] is used to cover the sample so that the directional high-speed ion can attack the polyimide at 45°. The aluminum mask is removed by aluminum etchant after dry etching, leaving a 45° slanted end surface on each end of the 48 fanouts of the waveguide. This 45° slanted end surface serves as the microcoupler. The SEM micrograph of the cross section of the 45° microcoupler is shown in Fig. 3. The 45° microcoupler at the end of the waveguide can be seen.

We have also developed an alternative approach to fabricate the H-tree waveguide and 45° surface-normal microcoupler using a double exposure method. In the double exposure method, the H-tree mask is placed over the sample and the lines of the H-tree mask are blocked using an additional "mask" which was slightly short at the end portions of the 48 branches that are exposed to 45°-slanted UV light. Then we

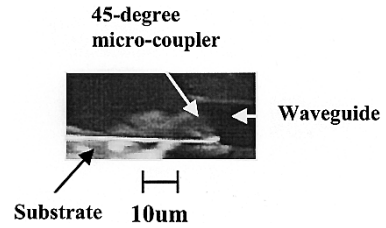

Fig. 3. The SEM micrograph of the cross section of the 45° microcoupler.

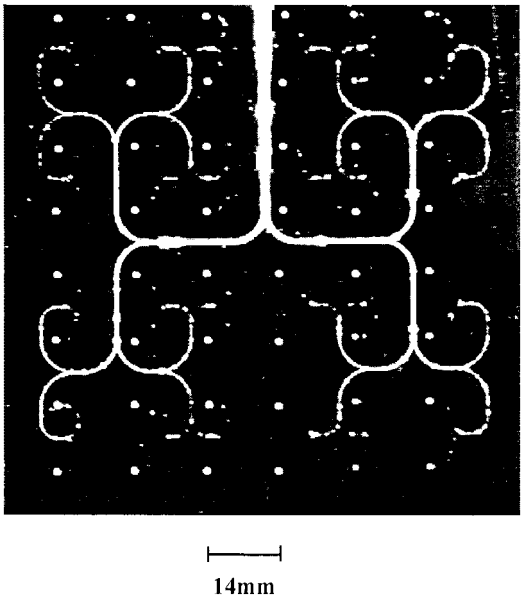

Fig. 4. Photograph showing the 48 surface-normal outputs.

block the end portions of the 48 branches using another "mask" and let the line portions of the H-tree waveguides be exposed to normal-incident UV light. The patterned waveguides were processed using standard polyimide development procedure leaving stable and moisture-resistant polyimide waveguides with 45° slanted ends after final bake.

III. Measurement and Theoretical Calculation

To demonstrate the functionality, butt coupling is used to couple the light into the waveguide. The surface-normal outputs from 48 output microcouplers can be seen in Fig. 4. However, the waveguide is also visible due to the high scattering loss at 633-nm wavelength. The 48 surface-normal outputs from the 45° microcouplers are shown. The waveguide loss is much lower when we use 850 nm wavelength. The output wavelength of the VCSEL is 850 nm and the surface-emitting characteristic of the VCSEL is a natural match to the 45° surface-normal microcoupler.

The output profiles from one of the 45° microcouplers are shown in Fig. 5(a)–(c). These figures correspond to $z = 100\ \mu$m, $z = 1$ mm, and $z = 5$ mm, respectively, where z is the distance from upper surface of the coupler to the point of observation. An estimate of output coupling efficiency was obtained by observing the propagation losses in the waveguide, and intensity profiles before and after the coupler, and coupled out beam. The estimated output coupling efficiency of this 45° microcoupler is nearly 100% and does not show noticeable change at 850-nm wavelength. The half-

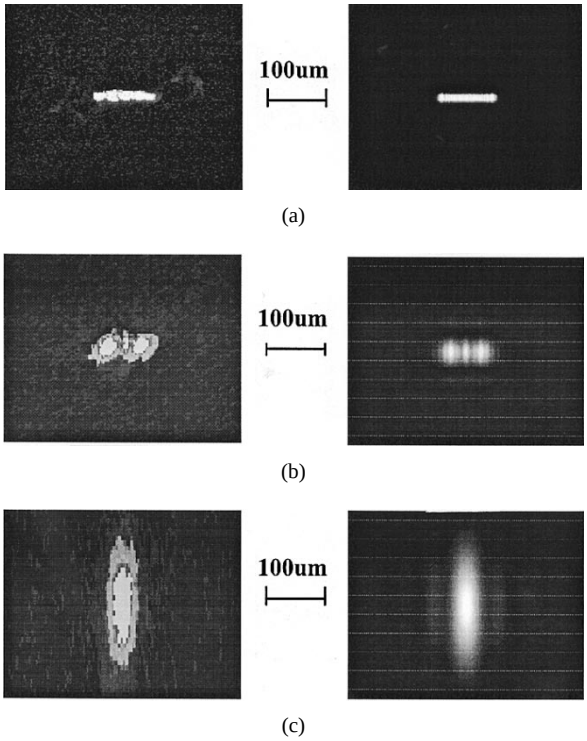

Fig. 5. The output profiles from the 45° surface-normal microcoupler. (a) $z = 100$ μm (experiment). (b) $z = 1$ mm (experiment). (c) $z = 5$ mm (experiment). (a′) $z = 100$ μm (theory). (b′) $z = 1$ mm (theory). (c′) $z = 5$ mm (theory).

width at half-maximum (HWHM) of the output profile at the microcoupler is about 60 μm, which is comparable or less than the active region of a typical fast photodetector having a bandwidth of 10 GHz [9], [10]. If the photodetectors are mounted close to the microcouplers, then most of the light can reach the photodetectors and thus the coupler-to-detector coupling efficiency can be very high.

The output profile from the 45° microcoupler can be determined using diffraction theory. According to Fresnel approximation [11], the near field distribution $U(x, y)$ is given by

$$U(x, y) = \frac{\exp(jkz)}{jz\lambda} \int_{-\infty}^{\infty} U(\xi, \eta) \cdot \exp\left\{ j \frac{k}{2z} [(x-\xi)^2 + (y-\eta)^2] \right\} d\xi \, d\eta$$

where $U(\xi, \eta)$ is the complex amplitude of the excitation at point (ξ, η) on the 45° microcoupler, $U(x, y)$ the complex amplitude of the observed field at point (x, y), k the magnitude of wave vector and z the distance from the upper surface of the 45° microcoupler to observing point. However, direct integration based on Fresnel approximation fails for a small z due to the fast oscillations of the Fresnel factor [12]. A modified convolution approach is used to calculate the $U(x, y)$ and the output profiles. The theoretical output profiles at $z = 100$ μm, $z = 1$ mm, and $z = 5$ mm from the 45° microcoupler are shown in Fig. 5(a′), (b′), and (c′), respectively. For these calculations, only the fundamental propagating mode of the waveguide was considered. Compared to Fig. 5(c′), the sidelobes in Fig. 5(c) is not clear due to the poor contrast of the image. As z becomes larger, the output light diverges faster in the direction that corresponds to the smaller dimension of the 45° microcoupler. Calculated and experimentally observed output profiles match very well. The simulation result considering the fundamental mode only, presented here is realistic because of the fact that in our highly multimode waveguides most of the energy remains confined to the fundamental and few lowest order modes. However, detailed study including the effect on the coupling efficiencies of higher modes and different claddings is underway that will be reported soon in a separate paper.

In summary, the 45° microcouplers in guided-wave optical clock distribution system have been investigated. Both RIE and double exposure method were used to fabricate the 45° microcouplers. The 1-to-48 surface-normal output coupling is demonstrated. The output coupling efficiency is nearly 100%. The final planarization step involving top cladding layer and the integration of VCSEL and photodetectors with an H-tree waveguide and 45° microcouplers are in progress. The high efficiency of surface-normal coupling is an obvious advantage when the optical clock distribution system is integrated with lasers and photodetectors for intrachip, interchip, and interboard interconnects.

REFERENCES

[1] R. T. Chen, L. Wu, F. Li, S. Tang, M. Dubinovsky, J. Qi, C. L. Schow, J. C. Campbell, R. Wickman, B. Picor, M. Hibbs-Brenner, J. Bristow, Y. S. Liu, S. Rattan, and C. Nodding, "Polyimide-based waveguides for guided-wave multi-GBit/sec MCM optoelectronic interconnects," in *Critical Review on Sol-Gel and Polymer Photonic Devices*, vol. CR-68, pp. 228–249, 1997.

[2] R. Chen, "Polymer-based photonic integrated circuits," *Opt. Laser Technol.*, vol. 25, no. 6, pp. 347–365, 1993.

[3] R. Chen, H. Lu, D. Robinson, M. Wang, G. Savant, and T. Jannson, "Guided-wave planar optical interconnects using highly multiplexed polymer waveguide holograms," *J. Lightwave Technol.*, vol. 10, pp. 888–897, July 1992.

[4] J. Cook, G. Este, F. Shepherd, W. Westwood, J. Arrington, W. Moyer, J. Nurse, and S. Powell, "Stable low-loss optical waveguides and micromirrors fabricated in acrylate polymers," *Appl. Opt.*, vol. 37, pp. 1220–1226, 1998.

[5] R. Waldhausl, B. Schnabel, P. Dannberg, E. Kley, A. Brauer, and W. Karthe, "Efficient coupling into polymer waveguides by gratings," *Appl. Opt.*, vol. 36, pp. 9383–9390, 1997.

[6] J. Miller, N. de Beaucoudrey, P. Chavel, J. Turunen, and E. Cambril, "Design and fabrication of binary slanted surface-relief gratings for a planer optical interconnection," *Appl. Opt.*, vol. 36, pp. 5717–5727, 1997.

[7] G. D. Boyd, L. A. Coldren, and F. G. Storz, "Directional reactive ion etching at oblique angles," *Appl. Phys. Lett.*, vol. 36, no. 7, pp. 583–585, 1980.

[8] L. Wu, B. Bihari, J. Gan, R. T. Chen, and S. Tang, "Board level optical clock signal distribution using Si-CMOS compatible polyimide-based 1-to-48 fanout H-tree," in *Proc. SPIE, Integrated Optoelectronics*, 1998, vol. 3551, pp. 95–101.

[9] J. C. Campbell, "Photodetectors for optoelectronic integrated circuits," in *Integrated Optoelectronics*, M. Dagenais, R. F. Leheny, and J. Crow, Eds. New York: Academic, 1995, ch. 11, pp. 419–444.

[10] Data sheet, Hamamatsu G4176 series photodetectors.

[11] J. W. Goodman, *Fourier Optics*, 2nd ed. New York: McGraw-Hill, 1996, ch. 4, pp. 63–89.

[12] M. Sypek, "Light propagation in the fresnel region. New numerical approach," *Opt. Commun.*, vol. 116, no. 1–3, pp. 43–48, 1995.